

Computational Investigations on the Binding Mode of Ligands for the Cannabinoid-Activated G Protein-Coupled Receptor GPR18

Alexander Neumann,^{1,2} Viktor Engel,¹ Andhika B. Mahardhika,^{1,2} Clara T. Schoeder,^{1,2} Vigneshwaran Namasivayam,¹ Katarzyna Kieć-Kononowicz,³ and Christa E. Müller^{1,2*}

¹ PharmaCenter Bonn, Pharmaceutical Institute, Pharmaceutical Sciences Bonn (PSB), Pharmaceutical & Medicinal Chemistry, University of Bonn, Bonn 53121, Germany

² Research Training Group 1873, University of Bonn, Bonn 53127, Germany

³ Department of Technology and Biotechnology of Drugs, Faculty of Pharmacy, Jagiellonian University Medical College, Medyczna 9, 30 - 688 Krakow, Poland.

* Correspondence: christa.mueller@uni-bonn.de; Tel.: +49-228-73-2301. Fax: +49-228-73-2567

Table of Contents

Figure S1. Multiple sequence alignment of GPR18 for homology modeling.....	2
Figure S2. Time scale of the molecular dynamics simulation of antagonist 4	3
Figure S3. Time scale of the molecular dynamics simulation of antagonist 5	4
Figure S4. Trajectories of salt bridges.....	5
Figure S5. Possible interaction of antagonist 6 with Asn185.....	6
Figure S6. Structures of GPR18 imidazothiazinone antagonists	7
Figure S7. Structures of GPR18 antagonists with modification of the core structure	8
Figure S8. Comparison of the binding modes of antagonists 5 and 32	9
Figure S9. Multiple sequence alignment of human GPR18 and the cannabinoid receptors CB ₁ and CB ₂	10
Figure S10. Comparison of the binding mode of THC to GPR18 with the binding of THC derivatives to the CB ₁ receptor.....	11
References	12

4xnv	1	TGFQF-YYLPAVYILVFIIGFLGNSVAIWMFVFHMKPWG SIVSYM FNLALADFLYVL TLP	59
5c1m	1	PSMVTAITIMALYSIVCVVGLFGNFLVMYVIVRYTKMKTATNIYIFNLALADALATSTLP	60
5xsz	1	DNFKYPLYSM-VFSIVFMVGLITNVAAAMYIFMC SIKLRNETTTYMMNLVVS DLLFVLTLP	59
GPR18	1	--DEYKIAALVFYSCIFIIGLFVNITALWVFSCTTKRTTVTIYMMNVALVDLIFIMTLP	58
4xnv	60	ALIFYYYFNKTDWIFGDAMCKLQRFFHVNLGSILFLTCISAHRYSGVVYP-KSLGR LKK	118
5c1m	61	FQSVNYLMGT-WPFGN ILC KIVISIDYYNMFTSIFTLCTMSVDRYIAVCHPVKA LDFRTP	119
5xsz	60	LRVFYFVQQN-WPFGSLLC KLSVSLFYTNMYGSILFLTCISVDRFLAIVYPFRSRGLRTK	118
GPR18	59	FRMFYYAKDE-WPFG EYFC QILGALT VFP SIALWLLAFISADRYMAIVQP KYAKELKNT	117
4xnv	119	KNAICISVLVWLIVVVAISPILFY-SGTGVRKNKTITCYDTSDEYLRSYFIYSMCTTV-	176
5c1m	120	RNAKIVNVNCNWISSAIGLPVMFM--ATTKYRQGSIDCTLTFSHPTWYWE NLLKICVFI-	176
5xsz	119	RNAKIVCAAVVVLVLSGS LPTGFMLNSTNKLENN SISCF-----EWK-SHLSKV VIFIE	171
GPR18	118	CKAVLACVG VVWIMTLTTTPLL LLYKDPDK-DSTPATCLKISDIIYLKAVNVNLTRLT-	175
4xnv	177	-AMFCVPLVLIILGCYGLIVRALIYKEPL-----RRKSIYLVIIIVLTVFAVSYIPFH	226
5c1m	177	-FAFIMPVLIITVCYGLMILRLKSVRMLSGSKEKDRNLRRIRTRMVL VVVA FIVCWTPIH	235
5xsz	172	TVGFLIPLMLNVVCSAMVLQTLRRPNTV-----NKKKILRMIIVHLFIFCFCFIPYN	224
GPR18	176	-FFF LIPLFIMIGCYLVIIHNLLHGRTSK--LKPKVKEKSIR III ITLLVQLVCFMPFH	231
4xnv	227	VMKTMNLRARLDFQTPAMCAFNDRVYAT-YQVTRGLASLN S C VN P ILYFLAGDTFRRR	283
5c1m	236	I--YVI IKALI---TIP----ETTFQTVSWHFCIALGYTN S CLNPVLYAFLDENFKRC	284
5xsz	225	V--NLVFYSLVRTNTLKGCAAESVVRTI-YPIALCIAVSNCCFDPIVYYFTSETIQNS	279
GPR18	232	I--CFAFLMLGT-----GENSYNPWG AFTFLMN LSTCLDV ILYYIVSKQFQAR	278

Figure S1. Multiple sequence alignment of the human GPR18 and the templates chosen for homology modeling.

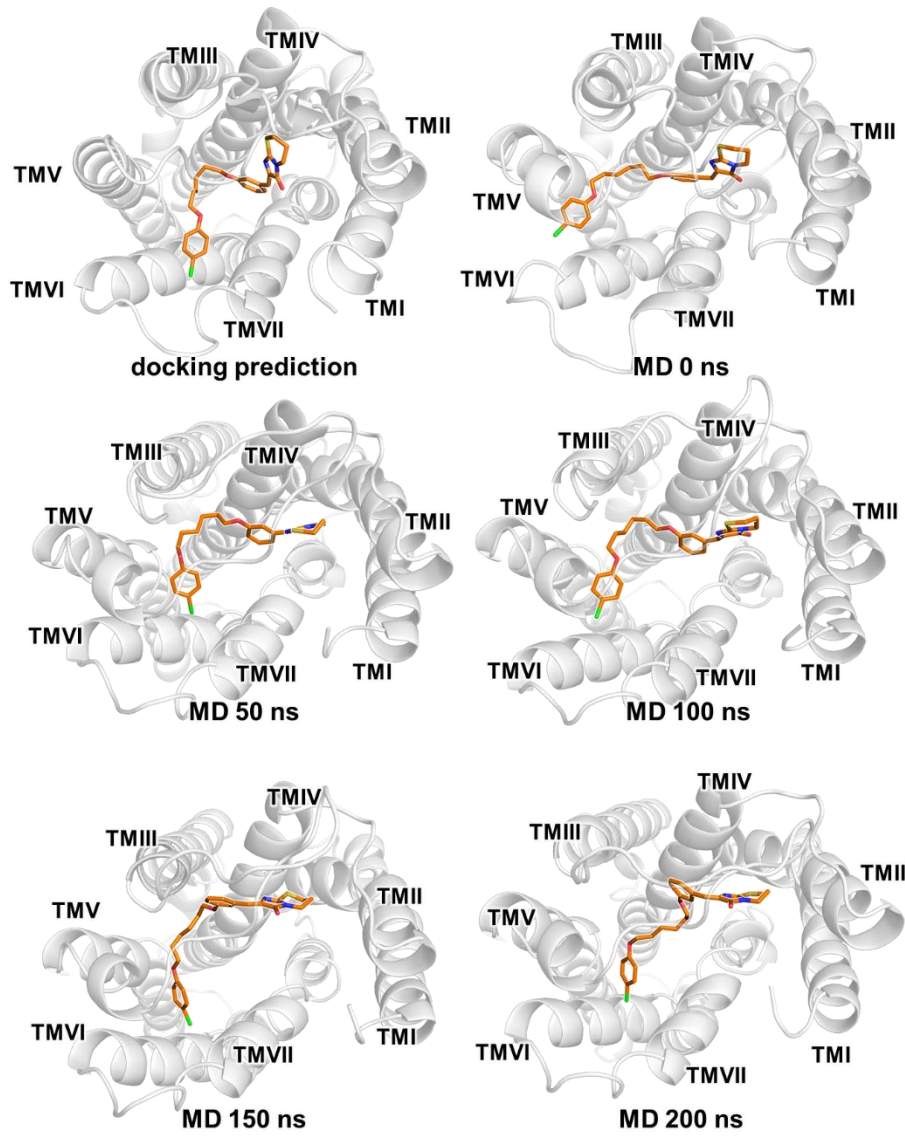


Figure S2. Time scale of the molecular dynamics (denoted 'MD') simulation of GPR18 homology model complex with antagonist 4. The docking prediction which was used for the simulation run is shown at the top left corner. 0 ns presents the complex after relaxation steps.

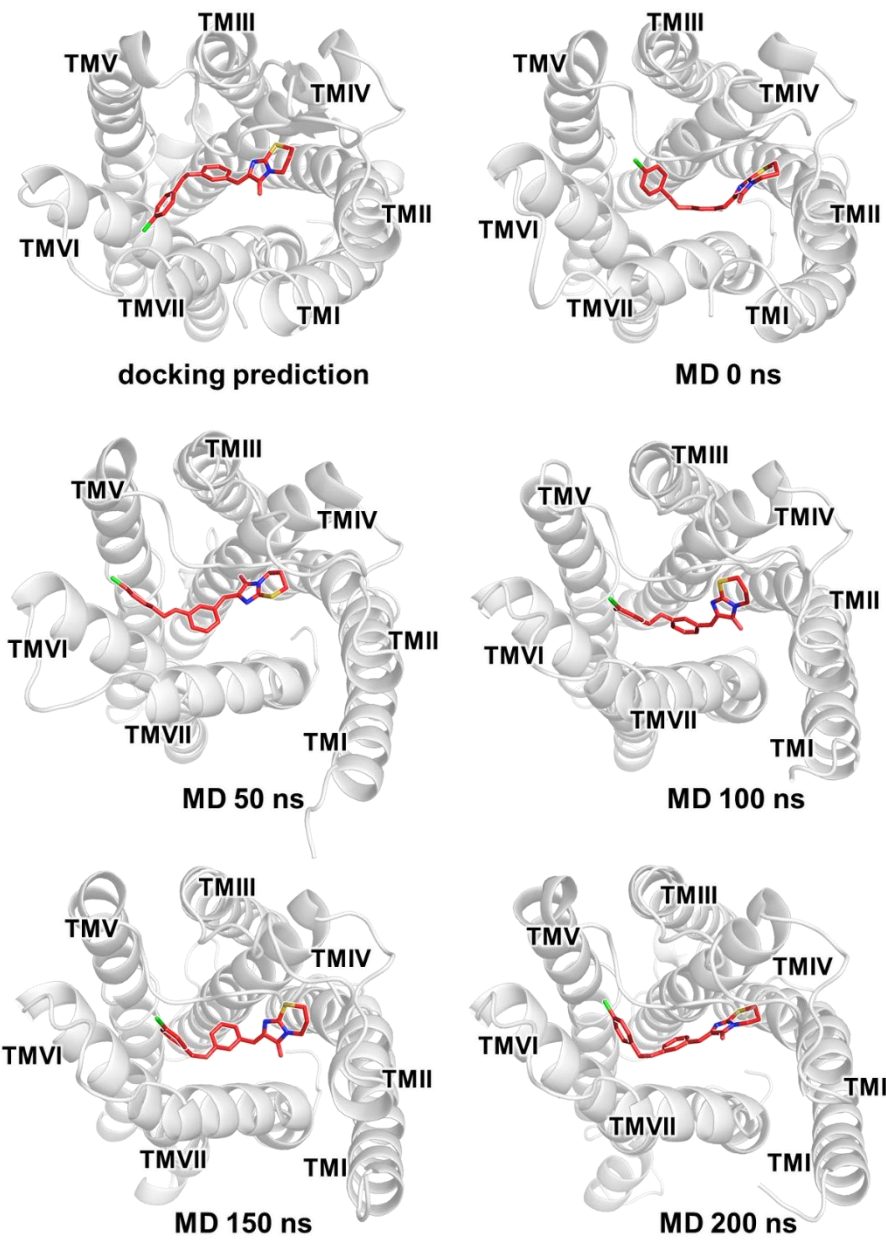


Figure S3. Time scale of the molecular dynamics (denoted 'MD') simulation of GPR18 homology model complex with antagonist 5. The docking prediction which was used for the simulation run is shown at the top left corner. 0 ns presents the complex after relaxation steps.

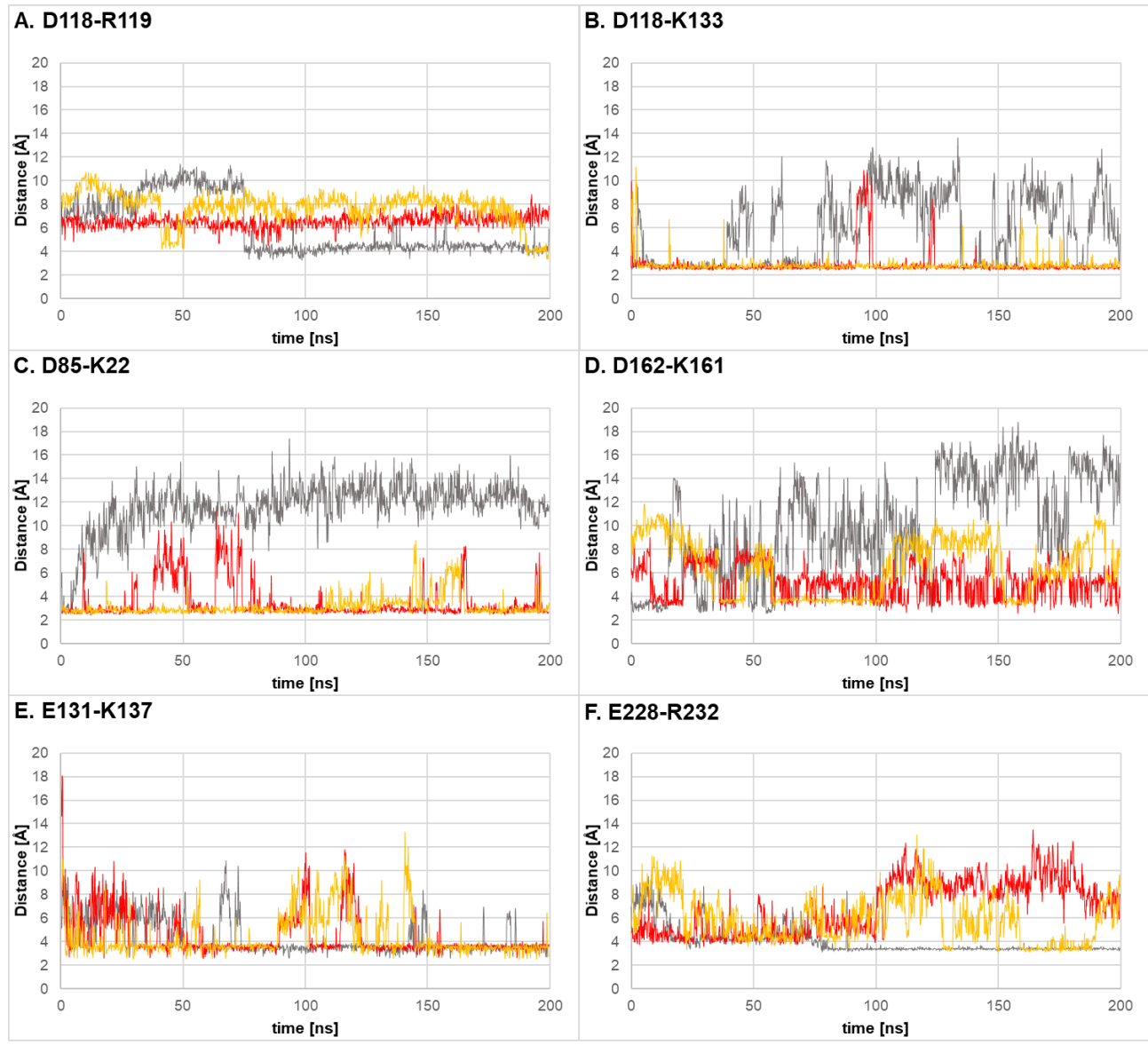


Figure S4. Trajectories of salt bridges during the 200 ns MD simulation runs.

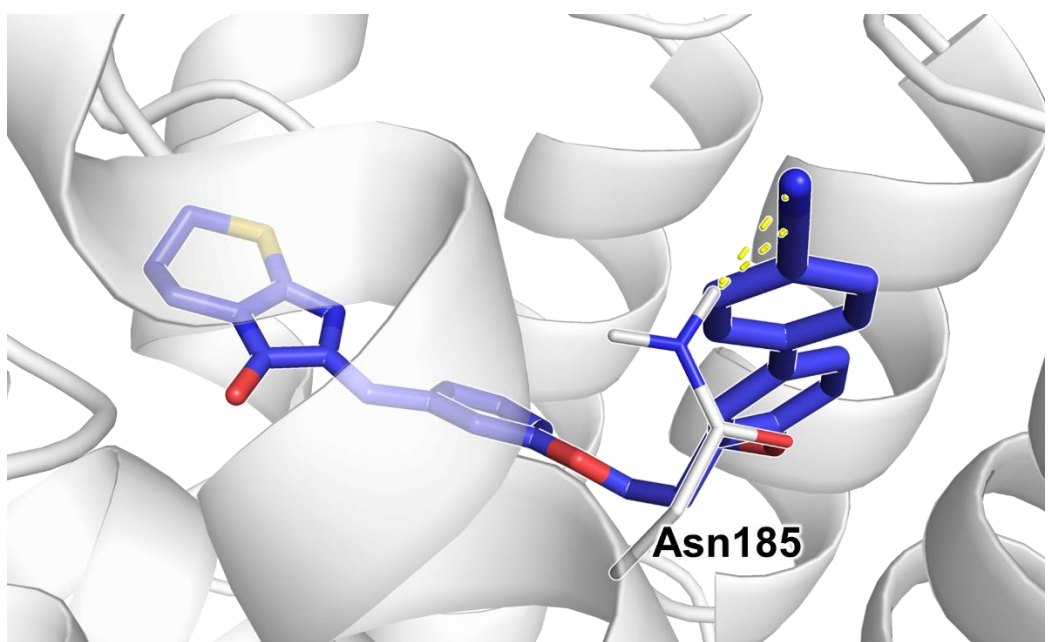


Figure S5. Possible interaction of antagonist 6 with a rotamer of Asn185.

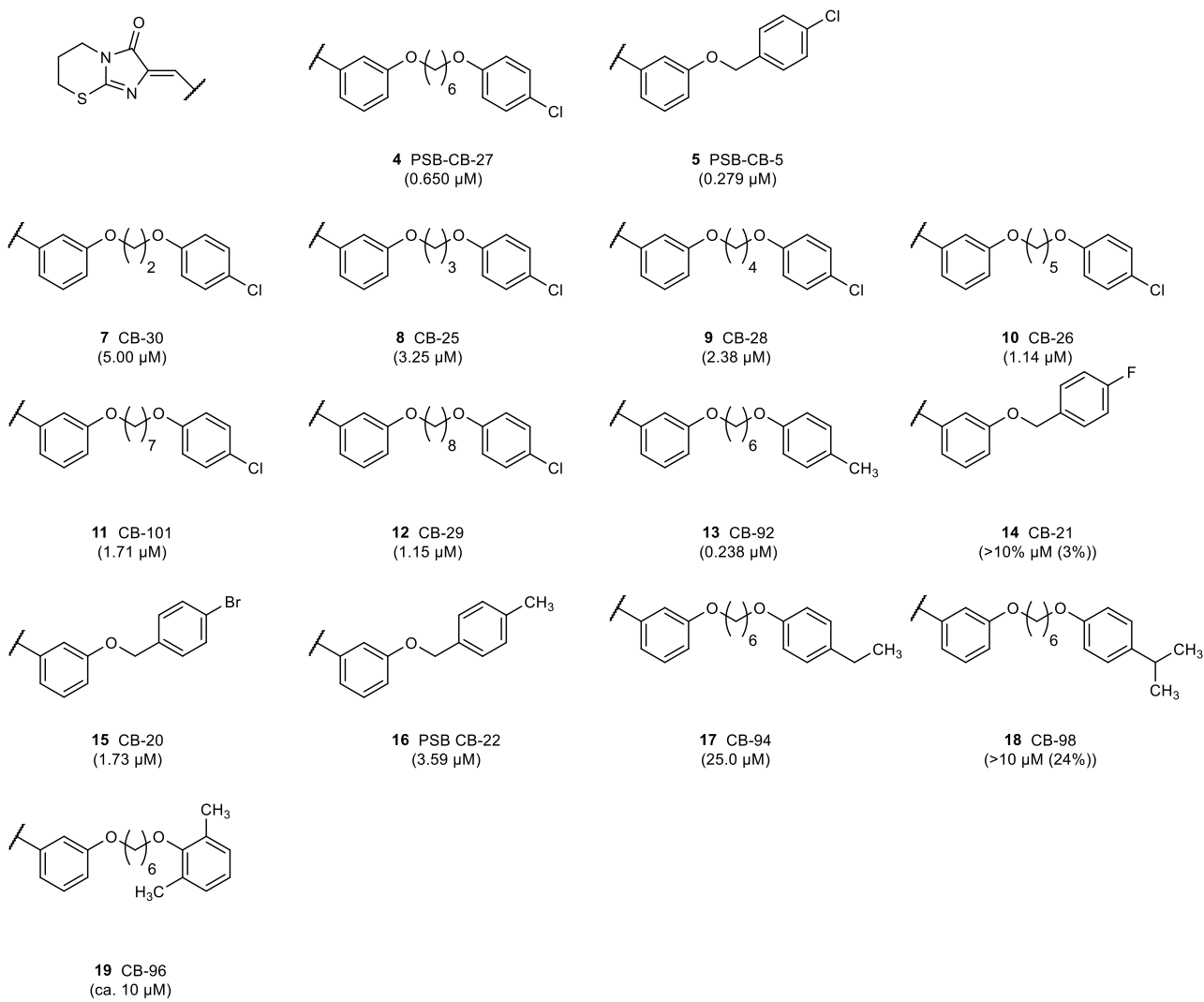


Figure S6. Structures of GPR18 imidazothiazinone antagonists with their respective IC_{50} values in brackets. For IC_{50} values $> 10 \mu\text{M}$ the percent inhibition of agonist-induced luminescence signal at $10 \mu\text{M}$ is given. Biological results were taken from published studies [1].

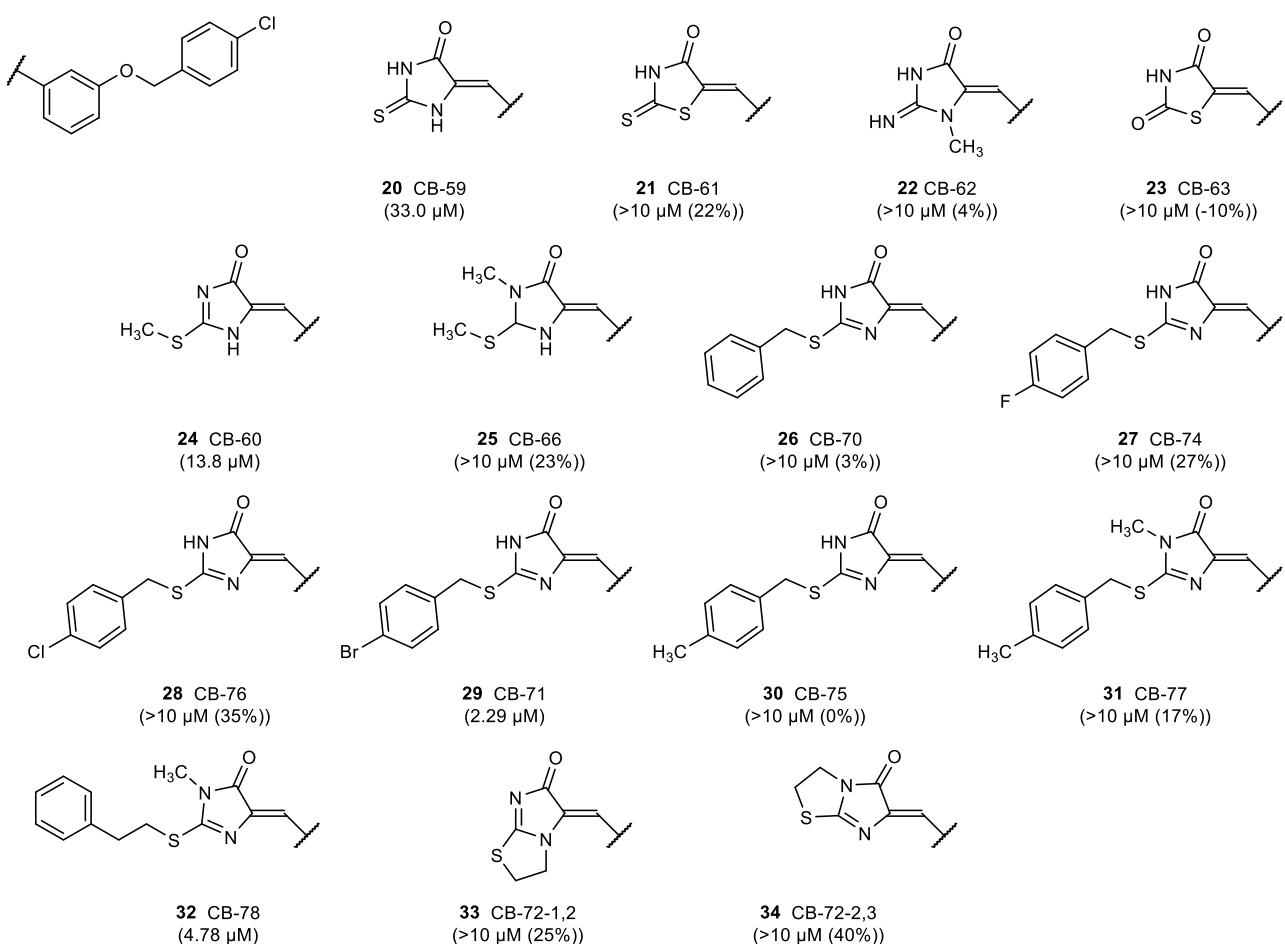


Figure S7. Structures of GPR18 antagonists with modification of the core structure with their respective IC_{50} values in brackets. For IC_{50} values $> 10 \mu\text{M}$ the percent inhibition of agonist-induced luminescence signal at 10 μM is given. Biological results were taken from published studies [1].

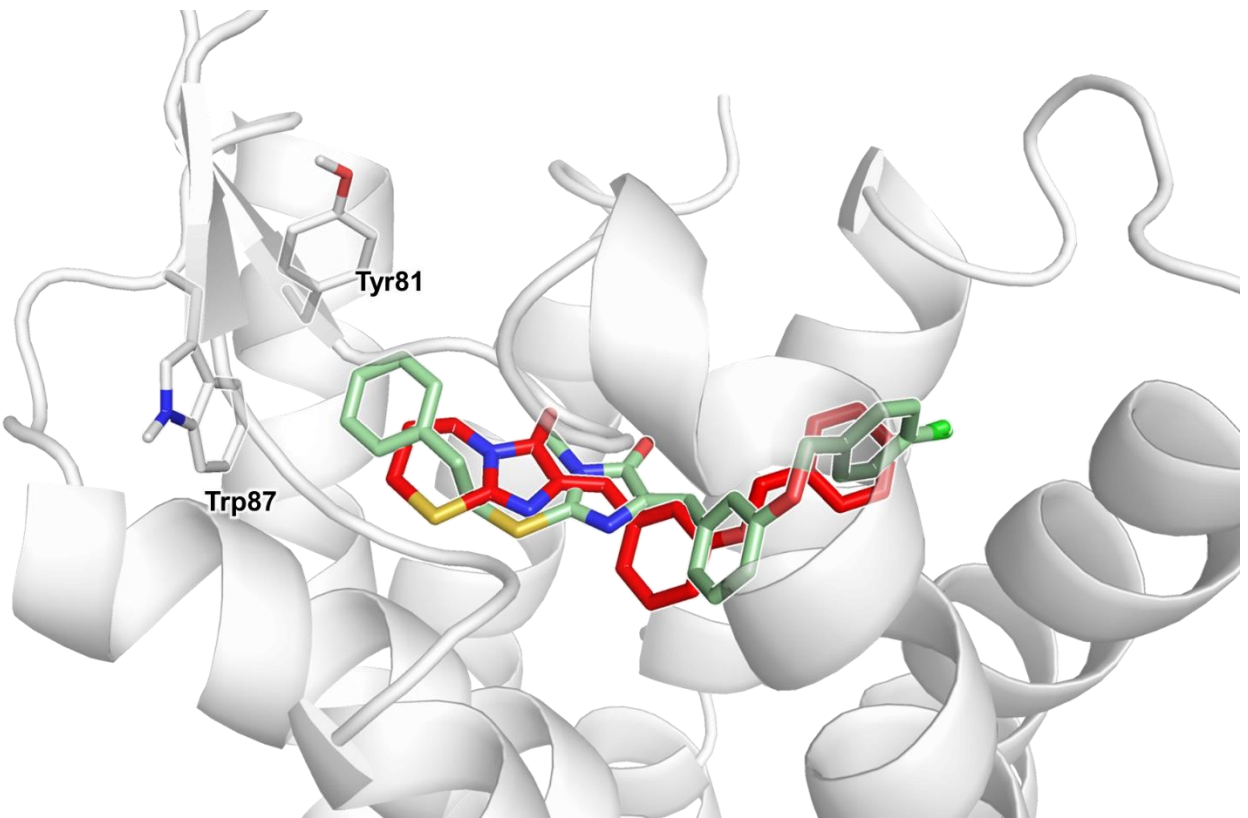


Figure S8. Comparison of the putative binding mode of antagonist 32 (green) and predicted binding mode of antagonist 5.

sp Q14330 GPR18_HUMAN	MKSILDGLADTTFRITTDLLYVGSNDIQYEDIKGDMASKLGYFPQKFPLTSFRGSPFQE	0
sp P21554 CNR1_HUMAN		60
sp P34972 CNR2_HUMAN		0
		TMI
sp Q14330 GPR18_HUMAN	MITLNNQDQPVPFNS-----SHPDEYKIA	24
sp P21554 CNR1_HUMAN	KMTAGDNPQLVPADQVNITEFYNKSLSSFKENEENIQCGENFMDIECFMVNLNPSQQLAIA	120
sp P34972 CNR2_HUMAN	-----MEECWVT-----EIAANGSKDGLDSNPMKDYMILSGPQKTAVA37	
		TMII
sp Q14330 GPR18_HUMAN	ALVFYSCIFIIGLFVNIT---ALWVFSCTTK-KRTTVTIYMMNVAVLDI---FIMTFL	75
sp P21554 CNR1_HUMAN	VL-----SLTLGTFVLENLLVLCVILHSRSLRCRPSYHFIGSLAVADLLGSVIFVYSFI	175
sp P34972 CNR2_HUMAN	VL-----CTLLGLLSALENVAVLYLILSSHQLRRKPSYLFIGSLAGADFLASVVFACSFV	92
	.	:
	*	:
	TMIII	
sp Q14330 GPR18_HUMAN	FDFRMFYAKDEWPFGHEYFCQIIGAAT-VFYPSTIALWLLAFISADRYMAIVQPKYAKELKN	134
sp P21554 CNR1_HUMAN	DHFVFRHR-KDS---RNVFLFKGGT-TASFTASVGS--LFLTAIDRYISIHRPLAYKRIVT	229
sp P34972 CNR2_HUMAN	DHFVFG-H-VDS---KAVFLLKGGT-TMTFTASVGS--LLLTAAIDRYLCLRYPPSYKALLT	146
	*	:
	*	.
	*	*
	*	*
	TMIV	
sp Q14330 GPR18_HUMAN	TCKAVLACVGWIMTLTTTPLLLYKDPDKDSTPATCLKIDIIYLKAVNVNLTRLTF	194
sp P21554 CNR1_HUMAN	RPKAVVAFCLMWTTIAIVIAVPLLGWNCEK---LQSVCSDIYPHI-----DETLYLMF	278
sp P34972 CNR2_HUMAN	RGRALVTLGIMWMVLSALVSYLPILMGWTCCP---RPCSELVPLI-----PNDYLLS	193
	*	:
	*	:
	*	:
	*	:
	TMV	
sp Q14330 GPR18_HUMAN	FFLIPPLFIMIG---CYLV-----IIHNLLHGRTSKLKPVKEKS	230
sp P21554 CNR1_HUMAN	WIGVTSVLLLFIVYAYMILWKAHSHAVRMIQRGTQKSIIHTSEDGKVQVTRPDQARMD	338
sp P34972 CNR2_HUMAN	WLLFIAFLFSGIIYTGHVLWKAHQHVASLSGH-----QDRQVPGMARMRLD	240
	:	:
	:	*
	TMVI	
sp Q14330 GPR18_HUMAN	IR---IIITLLVQVLVCFMPFHICFAFLMLGTGENSYNPWFATTFLMLNSTCLDVILYY	287
sp P21554 CNR1_HUMAN	IRLAKTLLVLLVVLIIICWGPFLAIMVYDVGKMNKLTKTVCAFCSMLCLLNSTVNPIIYA	398
sp P34972 CNR2_HUMAN	VRLAKTLLGVLVAVLPLICWPFPLALMAHSLATTLSQVKKACAFCSMLCLINSMVNPVIYA	300
	*	:
	**	:
	**	:
	**	:
	TMVII	
sp Q14330 GPR18_HUMAN	IVSKQFQARVISVMLYRNLYLRSMRRKSFRSGSLRSLSNINSEML-----	331
sp P21554 CNR1_HUMAN	LRSKDLRHAFRSMFP---SC-----EGTAQPLDNMSGD---SDCLHKHANN---	438
sp P34972 CNR2_HUMAN	LRSGEIRSSAHCL---HW-----KKCVRGLGSEAKEEAPRSSVTETEADGKITP	348
	:	*
	:	..
	:	:

Figure S9. Multiple sequence alignment of human GPR18 and the cannabinoid receptors CB₁ and CB₂. Residue positions involved in the binding of cannabinoid agonists in the X-ray crystal structure of CB₁ receptor are highlighted.

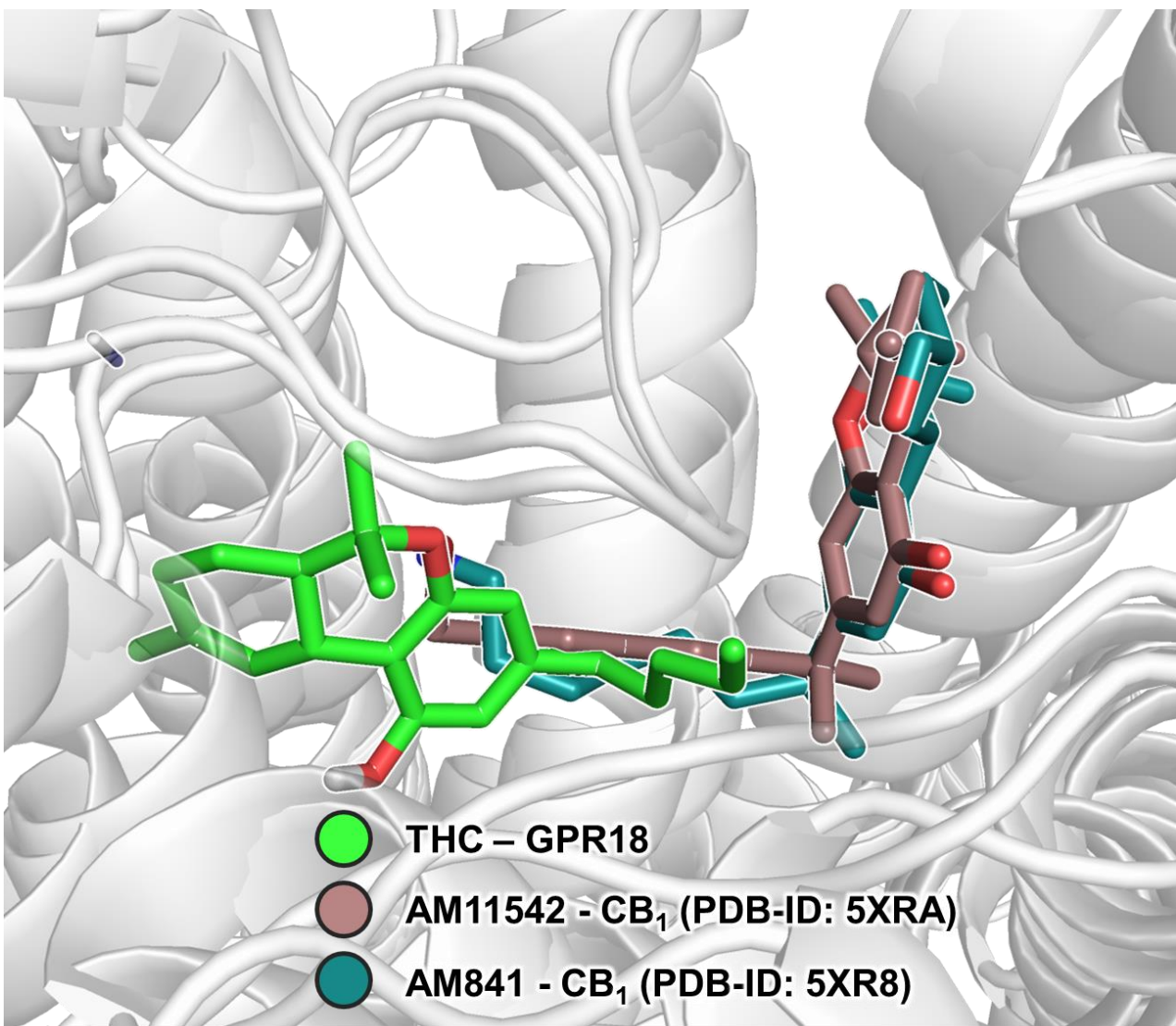


Figure S10. Comparison of the proposed binding mode of THC to GPR18 with the binding of THC derivatives to the CB₁ receptor as observed in the crystal structure [2].

References

1. Schoeder, C. T.; Kaleta, M.; Mahardhika, A. B.; Olejarz-Maciej, A.; Łażewska, D.; Kieć-Kononowicz, K.; Müller, C. E. Structure-activity relationships of imidazothiazinones and analogs as antagonists of the cannabinoid-activated orphan G protein-coupled receptor GPR18. *Eur. J. Med. Chem.* **2018**, *155*, 381–397.
2. Hua, T.; Vemuri, K.; Nikas, S. P.; Laprairie, R. B.; Wu, Y.; Qu, L.; Pu, M.; Korde, A.; Jiang, S.; Ho, J.-H.; *et al.* Crystal structures of agonist-bound human cannabinoid receptor CB1. *Nature* **2017**, *547*, 468–471.